

The multi-frequency parsec-scale structure of PKS 2254–367 (IC 1459): a luminosity-dependent break in morphology for the precursors of radio galaxies?

S.J. Tingay^{1*} and P.G. Edwards^{2†}

¹*International Centre for Radio Astronomy Research, Curtin University, Bentley, WA 6102, Australia*

²*Australia Telescope National Facility, CSIRO Astronomy and Space Science, Epping, NSW 1710, Australia*

Submitted: 2014

ABSTRACT

We present the first multi-frequency VLBI images of PKS 2254–367, a Giga-hertz-Peaked Spectrum (GPS) radio source hosted by the nearby galaxy IC 1459 ($D=20.5$ Mpc). PKS 2254–367 and the radio source in NGC 1052 (PKS 0238–084; $D=17.2$ Mpc) are the two closest GPS radio sources to us, far closer than the next closest example, PKS 1718–649 ($D = 59$ Mpc). As such, IC 1459 and NGC 1052 offer opportunities to study the details of the pc-scale radio sources as well as the environments that the radio sources inhabit, across the electromagnetic spectrum. Given that some models for the origin and evolution of GPS radio sources require a strong connection between the radio source morphology and the gaseous nuclear environment, such opportunities for detailed study are important. Our VLBI images of PKS 2254–367 show that the previously identified similarities between IC 1459 and NGC 1052 continue onto the pc-scale. Both compact radio sources appear to have symmetric jets of approximately the same luminosity, much lower than typically noted in compact double GPS sources. Similarities between PKS 2254–367 and NGC 1052, and differences with respect to other GPS galaxies, lead us to speculate that a sub-class of GPS radio sources, with low luminosity and with jet-dominated morphologies, exists and would be largely absent from radio source surveys with ~ 1 Jy flux density cutoffs. We suggest that this possible low-luminosity, jet-dominated population of GPS sources could be an analog of the FR-I radio galaxies, with the higher luminosity lobe-dominated GPS sources being the analog of the FR-II radio galaxies.

Key words: galaxies: active — galaxies: individual: PKS 2254–367 (IC 1459) — techniques: high angular resolution

1 INTRODUCTION

Giga-hertz-Peaked Spectrum (GPS) sources represent at least 10% cent of the bright radio source population (O’Dea 1998) and are thought to represent the early evolutionary stages of the FR-II, and perhaps FR-I, radio galaxies (e.g., Snellen et al. 2003). High angular resolution studies are therefore of great importance for understanding the early stages of their evolution, particularly for low-redshift GPS galaxies where high angular resolution corresponds to high linear resolution. Multi-frequency observations additionally allow the spectral index distribution to be studied: flat or inverted spectra identify regions of active particle acceleration, whereas steeper spectra are consistent with an aging

population of relativistic electrons (although these interpretations can be complicated in high density regions by the effects of absorption).

Multi-frequency, multi-epoch observations with the Australia Telescope Compact Array (ATCA) (Tingay et al. 2003a) established PKS B2254–367 as a GPS source. In addition to the peaked radio spectrum, PKS B2254–367 displays all of the typical characteristics of GPS sources, with compact structure seen on the maximum ATCA 6 km baselines, low fractional polarisation, and low variability over the 3.5 year period of the ATCA monitoring (Tingay, Edwards & Tzioumis 2003b; Edwards & Tingay 2004). In general, GPS objects have marginal variability, representing the variations due to the evolution of a jet originating from a black hole and accretion disk system. In GPS objects, the contribution to the total flux density of the jet is small in fractional terms, leading to low levels of variability. Long

* E-mail: s.tingay@curtin.edu.au

† E-mail: Philip.Edwards@csiro.au

term gradual flux density variability has been reported for OQ208 (Wu et al. 2013). PKS2254–367 has a more irregular variability, similar to high frequency peaking GPS objects (e.g. Orienti, Dallacasa & Stanghellini (2007) and references therein). Observations at 20 GHz (Murphy et al. 2010) and 95 GHz (Sadler et al. 2008) confirm the PKS 2254–367 spectral index steepens beyond 8.6 GHz (the highest frequency of the original ATCA observations).

Assuming a Hubble constant of $75 \text{ kms}^{-1}\text{Mpc}^{-1}$ and correcting for the motion of our Galaxy in the direction of PKS 2254–367 relative to the Cosmic Microwave Background, the PKS 2254–367 redshift (0.006011, Zwaan et al. (2004)) indicates a distance of 20.5 Mpc. PKS 2254–367 is therefore one of the closest known GPS radio sources. NGC 1052 ($z=0.005037$) at 17.2 Mpc and PKS 1718–649 (NGC 6328: 0.014428) at 59 Mpc, in the same frame of reference, are the only two other GPS radio sources within 100 Mpc, for which the detailed kinematics of the host galaxies can be studied (see, e.g., Labiano et al. 2007). All three galaxies present strong evidence for merger activity, an actively fuelled black hole, and high density environments with which the radio sources interact (Tingay et al. 2003b).

The host galaxy of PKS B2254–367, IC 1459, is a giant elliptical galaxy in a loose group of spirals. IC 1459 is a LINER (Verdoes Kleijn et al. 2000), and has one of the strongest counter-rotating core components of any observed elliptical, suggestive of merger activity (Forbes, Franx, and Illingworth 1994). The dust distribution is irregular near the nucleus, indicating that infalling material may currently be fuelling the active nucleus (Forbes et al. 1994). The central black hole mass in IC 1459 is between $4 \times 10^8 M_{\odot}$ and $3 \times 10^9 M_{\odot}$ (Cappellari et al. 2002).

2 OBSERVATIONS AND RESULTS

Very Long Baseline Interferometry (VLBI) observations of PKS 2254–367 were made using the VLBA (excluding the northernmost stations at Brewster, North Liberty and Hancock) at frequencies of 1.655 and 4.975 GHz on 2003 November 29 and at frequencies of 2.266 and 8.416 GHz on 2003 December 11. Standard observing setups, with two-bit quantisation, were used.

The 1.7 and 5.0 GHz observations switched between these two bands on a 15 minute timescale over the 6 hour duration of the observation. A 32 MHz aggregate bandwidth was used at LCP. The 2.3 and 8.4 GHz observations used the dual “S/X” band receiver to record RCP. Switching between these frequencies was therefore not required, as both are available simultaneously. In this case, the aggregate bandwidth per band is half of that which is available for the 1.7 and 5.0 GHz observations, but the integration time is approximately doubled.

The data were correlated on the VLBA processor and initial standard data reduction was performed in AIPS, according to standard routines (amplitude calibration, instrumental phase and delay calibration, fringe-fitting etc). The data were then exported to DIFMAP (Shepherd 1997) for editing, imaging, and modelfitting of the (u, v) data.

The aims of imaging the data at the maximum possible angular resolution, to investigate the structure of the compact radio source, and to obtain quantitative information on

the spectral properties of the source structure, are difficult to achieve given the poor (u, v) coverage of the VLBA at southern declinations. The absence of Brewster, North Liberty, and Hancock from the array results in a large hole in a largely east-west (u, v) coverage. On the long baseline side of the hole are baselines to the Mauna Kea and St Croix antennas. On the short baseline side of the hole are baselines between the five antennas concentrated in the south west US.

A consequence of the (u, v) coverage is that approximately matched resolution images can be made at our four frequencies using a combination of restrictions on the (u, v) data and weighting of the visibilities (described in a sub-section below). This approach reveals useful qualitative information on the structure of the compact radio source. However, the uncertainties in deconvolution induced by the poor (u, v) coverage do not allow quantitative information on the spectral characteristics of the structure.

In order to best determine spectral information, the long baselines need to be discarded and restrictions on the short baseline (u, v) coverage are applied as a function of frequency to provide visibilities matched in spatial frequency (without the need for additional weighting) for component fitting in the (u, v) plane (described in a sub-section below).

Using these two approaches, we determine limited information on the structure and spectra of the compact radio source.

2.1 Approximately matched resolution imaging

In order to produce the highest angular resolution approximately matched images of the compact structure, we started with the full (u, v) coverage at 1.7 GHz. At 2.3 GHz, the same (u, v) coverage was used but a Gaussian taper giving a weight of 0.5 at a (u, v) distance of $20 \text{ M}\lambda$ (denoted 0.5, 20) was applied to produce an image which approximately matched the resolution obtained at 1.7 GHz. At 5.0 GHz, no Gaussian taper was used, but the long baselines to Mauna Kea to Saint Croix were removed, to approximately match the resolution at the two lower frequencies. At 8.4 GHz, the data on all baselines to MK and SC were also removed from the dataset and a Gaussian taper of 0.5, 30 was applied to the data, to approximately match the resolution at the other frequencies. All images were produced using uniform weighting of the data, image sizes of 256×256 pixels, and pixel sizes of 1.0 mas. Standard deconvolution and self-calibration routines were used to form the images. As phase referencing was not used for these observations, the self-calibration step in imaging (and indeed via fringe-fitting in AIPS), forces the brightest component in the image at the centre of the image. As seen below, the brightest component is the same component at all frequencies, thus the alignment of the images at the different frequencies is secure to first order. Small frequency-dependent shifts in the centroid of the brightest component are lost due to self-calibration. However, a comparison of the overall structure of the source allows a secure identification of the different components of emission across the different frequencies. These identifications are used to guide the model-fitting process described in the next section.

Table 1 lists the tapers used at each frequency, the di-

Table 1. Parameters of the images. The beam parameters are semi minor axis FWHM \times semi major axis FWHM @ beam position angle in degrees. (u, v) coverage refers to the full VLBA (Full) or without the baselines to Mauna Kea (–MK) or Saint Croix (–SC). Taper is described in the text. RMS is the Root Mean Square in the residual image pixels.

Parameter	1.7 GHz	2.3 GHz	5.0 GHz	8.4 GHz
Beam (mas \times mas @ PA $^\circ$)	3.3 \times 9.8 @ 0.0	3.4 \times 10.3 @ 0.5	3.5 \times 11.0 @ 4.9	3.2 \times 11.8 @ 11.2
(u, v) coverage	Full	Full	–MK, –SC	–MK, –SC
Taper (weight, uvdistance)	NA	0.5, 20	NA	0.5, 30
RMS (mJy/beam)	1.0	1.1	0.9	0.8

mensions of the resultant synthesised beams, and the image RMS values achieved.

Finally, all images were restored with a common Gaussian restoring beam of 3.5 mas \times 11 mas at a PA of 6.0 degrees and are shown in Figure 1. This procedure follows the imaging techniques used by Tingay & Murphy (2001).

2.2 Matched resolution model-fitting

As mentioned above, we seek to obtain limited spectral information on the compact radio source by discarding the longest baselines to Mauna Kea and St Croix and restricting the (u, v) coverages at all four frequencies to a range of 0–9 M λ . This allows the full short baseline (u, v) coverage at 1.7 GHz, and progressively more restricted coverages at the higher frequencies.

The 1.7 GHz dataset was fit with a model consisting of five circular Gaussian components, using the task modelfit in DIFMAP. We allowed the flux densities, positions, and sizes of the five components to vary until convergence. This model was then fit to the data at the three higher frequencies by keeping the positions and sizes of the five components constant and allowing the flux densities to vary. Good fits were found at all four frequencies using this method, providing integrated flux densities for each component in order to estimate the spectrum for each component. Model component types other than circular Gaussians were tested using this model-fitting approach and were not found to provide significantly better fits to the data. We justify the use of circular Gaussians as the simplest set of components that provide a good fit to the data with the minimum number of free parameters.

The errors on the VLBA flux density scale are approximately 5%. The model fit results for all four frequencies are given in Table 2 and the spectra are shown in Figure 2.

The results of the model-fitting are broadly consistent with the results of the imaging shown in Figure 1, discussed below.

3 DISCUSSION

The analysis above provides information on the structure and spectral properties of PKS 2254–367. As one of only a small number of GPS radio sources within 100 Mpc, it is important to determine the basic properties of the source and compare them to the other nearby, and more distant, GPS sources.

A point of interest is how the nearby GPS sources, such as PKS 2254–367, relate to the so-called compact symmetric

objects (CSOs). CSOs are compact (<1 kpc in projected extent) and have highly symmetric structures (Wilkinson et al. 1994); they are thought to be the progenitors of Fanaroff-Riley type II radio galaxies (Readhead et al. 1996). Snellen et al. (2004) show that a very high percentage of low redshift ($0.005 < z < 0.16$), compact ($< 2''$), and relatively weak (> 100 mJy at 1.4 GHz) radio sources associated with galaxies bright at optical wavelengths can be classified as GPS or CSS (compact steep spectrum) radio sources, and are, therefore, perhaps young radio galaxies.

We therefore examine PKS 2254–367 to determine how it relates to the classes of objects (GPS, CSS, CSO) thought to be the precursors of powerful radio galaxies, and in particular other nearby radio sources in these categories.

Tingay et al. (2003b) identified PKS 2254–367 ($D=20.5$ Mpc) as one of three low redshift GPS radio galaxies, along with PKS 1718–649 ($D=59$ Mpc) and NGC 1052 ($D=17.2$ Mpc). PKS 1718–649 has a so-called classical double morphology. Tingay et al. (2003b) listed a number of similarities between NGC 1052 and the host galaxy of PKS 2254–267 (IC 1459). Both galaxies have counter-rotating cores (Forbes et al. 1994; Bettoni et al. 2001) and LINER spectra (Verdoes Kleijn et al. 2000; Gabel et al. 2000). Both radio sources are predominantly compact and have peaked spectra (de Vries, Barthel, & O’Dea 1997; Tingay et al. 2003b). All three low redshift GPS sources support models in which a dense nuclear environment and merger activity are the cause for the mostly compact radio structure. PKS 2254–367 and NGC 1052 are hosted in cluster dominant (CD) elliptical galaxies.

Of the three bright components that dominate the pc-scale structure of PKS 2254–367, those labelled A, B, and C in Table 1, A has a marginally peaked spectrum, sits at the centre of the structure, is the brightest component, and is the most compact of the components. We therefore identify component A as likely to correspond to the nucleus of the radio source, presumably coincident with the supermassive black hole known to reside in the galaxy.

The pc-scale radio source therefore appears to be double-sided, with jet-like extensions comprised of the bright inner component B and the weaker outer component D towards the north-west, and the bright inner component C and the weaker outer component E towards the south-east. This structure is reflected in both the modelfitting results and the imaging results. The north-west components (B and D) have spectra that steepen above 2.3 GHz. The south-east components (C and E) have flat spectra. The spectra for the five components are shown in Figure 2.

PKS 2254–367 therefore seems to be a candidate CSO,

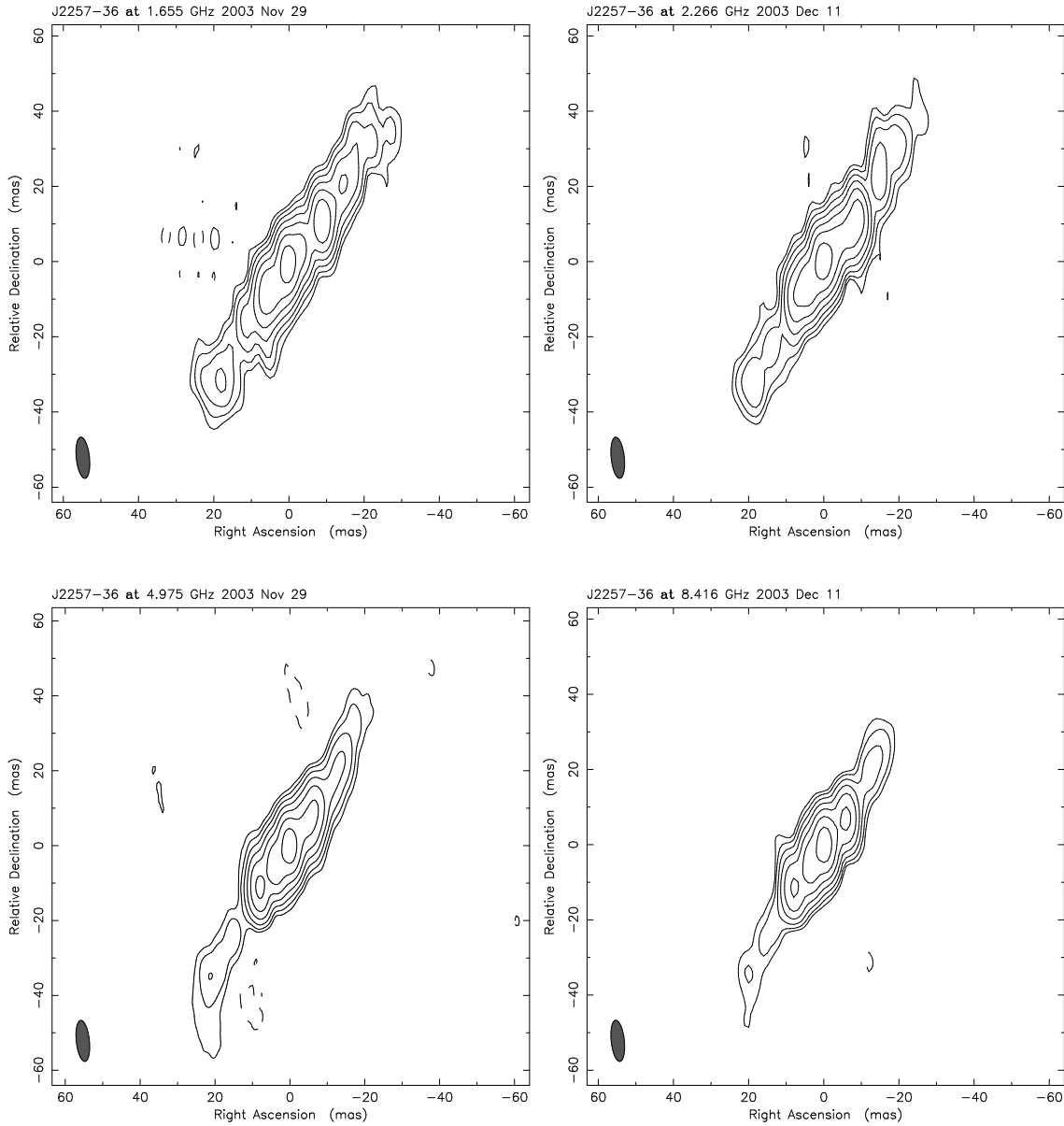


Figure 1. VLBA images of PKS 2254–367. All images have been restored with a beam of 11×3.5 mas at a position angle of 6° . The image peaks are 243, 262, 251 and 240 mJy/beam, at 1.7, 2.3, 5.0 and 8.4 GHz respectively. Contours are plotted at -1 (dashed), 1, 2, 4, 8, 16, 32, and 64% of the image peak.

Table 2. Flux densities of components fitted to (u, v) data in the range 0–9 M λ . S is the flux density (in Jy) of the model component at the frequency (in GHz) indicated by the subscript. r is the angular distance in milli-arcseconds of the component from the phase centre. θ is the position angle in degrees (east of north) of the component. a is the Full Width at Half Maximum of a circular Gaussian component (in milli-arcseconds)

Component	$S_{1.7}$	$S_{2.3}$	$S_{5.0}$	$S_{8.6}$	r	θ	a
A	0.49 ± 0.03	0.58 ± 0.03	0.53 ± 0.03	0.48 ± 0.03	1.6	-174	0.0
B	0.33 ± 0.02	0.30 ± 0.02	0.16 ± 0.01	0.10 ± 0.01	15.2	-42	7.3
C	0.17 ± 0.02	0.19 ± 0.02	0.17 ± 0.02	0.16 ± 0.02	16.2	149	6.9
D	0.08 ± 0.01	0.04 ± 0.01	< 0.03	< 0.03	40.9	-29	10.6
E	0.04 ± 0.01	0.05 ± 0.01	0.04 ± 0.01	0.05 ± 0.01	42.0	153	6.8

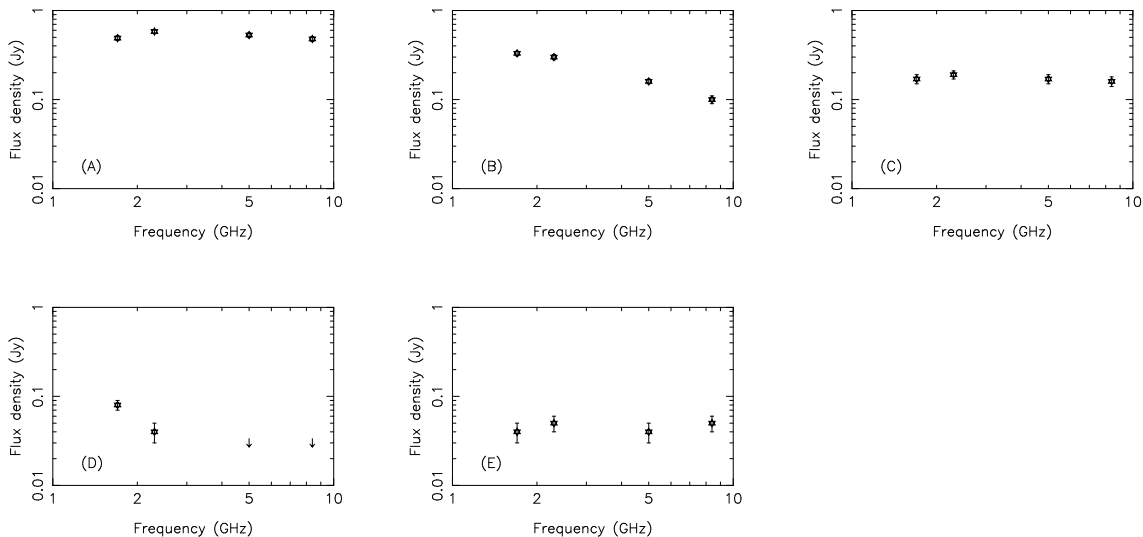


Figure 2. Spectra for the model fit components of Table 2.

with a symmetric structure centred on component A. In comparison to the CSO candidates found in the COINS survey (Peck and Taylor 2000), PKS 2254–367 seems most similar to the sources J0427+41 and J1546+00. Both these sources appear to have a strong core (more dominant than in PKS 2254–367, indicating that these cores may be beamed) and double sided jets. However, such sources make up a small minority of the candidates found by Peck and Taylor (2000). Orienti et al. (2004) report VLBA images of a sub-sample of CSS objects and out of 18 objects (from a parent sample of 87 objects), two have morphologies similar to PKS 2254–367, possibly without as strong a central core component (B3-VLA 1242+410 and B3-VLA 2358+406). Most candidate CSOs are dominated by strong edge-brightened lobes and have weak or absent jets and weak or absent cores. The more frequently observed morphology in the Peck and Taylor sample is more reminiscent of PKS 1718–649.

Our new VLBA data for PKS 2254–367 shows that similarities between PKS 2254–367 and NGC 1052 continue to be seen for the pc-scale radio source.

From comprehensive multi-epoch VLBI monitoring, NGC 1052 has been revealed to possess bi-directional jets with apparent speeds of up to $\sim 0.38c$ that appear to be orientated in the plane of the sky (Vermeulen et al. 2003; Lister et al. 2013). The jets in PKS 2254–367 also appear to be bi-directional, with a high degree of symmetry, although similar multi-epoch VLBI observations would be required to unambiguously demonstrate this through the detection of motion in the jet components. With a spacing between observing epochs of only 12 days, obviously no motion has been detected in PKS 2254–367 but the opposing jets appear highly symmetric with regard to their surface brightnesses, indicating that they are in the plane of the sky and/or not significantly relativistic.

The largest extent of the jets in NGC 1052 is approximately 3 pc (Vermeulen et al. 2003). In PKS 2254–367, the jets have a projected extent of approximately 8 pc.

The integrated monochromatic luminosity at 5 GHz of PKS 2254–367 is $\sim 7 \times 10^{22} \text{ W Hz}^{-1}$, and the compact radio source in NGC 1052 has a very similar luminosity, $\sim 5 \times 10^{22} \text{ W Hz}^{-1}$. PKS 1718–649 has a classical double morphology with an extent of 2 pc and a monochromatic luminosity at 5 GHz of $\sim 2 \times 10^{24} \text{ W Hz}^{-1}$ (Tingay et al. 1997). Unlike NGC 1052, no motion in the structure of PKS 1718–649 has been detected following multi-epoch VLBI observations, with an estimated upper limit on the separation speed of the double components of $0.08 c$ (Tingay et al. 2002).

In NGC 1052, Vermeulen et al. (2003) found strong evidence for free-free absorption within the central pc. We cannot examine this possibility for PKS 2254–367, since the limited frequency range, (u, v) coverage, and resolution of our data, compared to the NGC 1052 data, make detection of free-free absorption effects difficult. In general, distinguishing between free-free absorption and synchrotron self-absorption is difficult in GPS/CSO objects, as examined in detail by Tingay and de Kool (2003) for PKS 1718–649. More recent work on the absorption mechanism in PKS 1718–649 by Tingay et al. (2015) shows that free-free absorption is likely to be the cause of its spectral peak at $\sim 3 \text{ GHz}$.

The similarities between NGC 1052 and PKS 2254–367 on the pc-scale are interesting, as are the differences between these two sources and PKS 1718–649 and similar lobe-dominated GPS sources.

With the new images of PKS 2254–367, the two closest GPS sources are of low luminosity and have extended low-power jets (subluminal for NGC 1052, unknown for PKS 2254–367). The next closest sources are substantially more luminous – fifty times so in the case of PKS 1718–649 – and are dominated by powerful double morphologies (sometimes with weak cores and symmetric jets). PKS 2254–367 and NGC 1052 are below the lower edge of the distribution of luminosities of the sample of low redshift GPS and CSS

sources of Snellen et al. (2004), as all sources in that survey are more luminous than $\sim 10^{23} \text{ W Hz}^{-1}$ at 5 GHz. The objects with somewhat similar morphologies to PKS 2254–367 from Orienti et al. (2004) have luminosities substantially higher, of order $10^{27} \text{ W Hz}^{-1} h^{-1}$ at 400 MHz (these are CSS objects, with spectra still rising at 400 MHz).

We speculate that objects such as NGC 1052 and PKS 2254–367 represent a sub-class of GPS radio source which are compact, of low luminosity, and jet dominated. They are differentiated from many other GPS sources (such as PKS 1718–649) by the lack of powerful, compact lobes.

Such a possibility recalls the Fanaroff-Riley luminosity–morphology break seen in large-scale radio galaxies (Fanaroff & Riley 1974). The low luminosity radio galaxies (FR-I type) have prominent (two-sided or sometimes one-sided) jets and centre-brightened or indistinct radio lobes. The great majority of the higher luminosity radio galaxies (FR-II type) are dominated by edge-brightened lobes. They typically have apparently weak cores and weak jets. The apparent weakness of the jets is ascribed to relativistic beaming along the jet direction.

NGC 1052 and PKS 2254–367 may be the low-luminosity, jet-dominated analogs of FR-I type radio galaxies. Objects like PKS 1718–649 may be the higher luminosity analog of FR-II type radio galaxies. A possible implication of such a luminosity–morphology break could be that the origin of the difference between FR-I and FR-II type radio galaxies lies on the sub-parsec-scale, where the jet is formed close to the black hole and accretion disk. Such schemes are favoured in the theoretical models of Meier et al. (1997), who suggest that the FR-I/FR-II break is due to the magnetic field strength near the black hole.

However, other explanations may exist for the morphology of NGC 1052 and PKS 2254–367. The nuclear environment is thought to play a major role in the appearance and evolution of GPS radio sources, and this seems likely in the case of these two objects. In this case, the sub-pc environment of the black hole and accretion disk system would not be of primary relevance. Support for this view can be found in the fact that the properties of the pc-scale jets in FR-I and FR-II objects, as seen with VLBI, are indistinguishable in terms of morphology and apparent speed, for example as reported by Giovannini et al. (2001).

Very few sources like PKS 2254–367 or NGC 1052 have been studied in detail since even doubling their distance to a modest $\sim 40 \text{ Mpc}$ would mean that they lie a factor of four below the 1 Jy cutoff that is typical of previous radio source surveys. Multi-frequency surveys of weak radio sources would be required to find such objects. Beyond $\sim 50 \text{ Mpc}$ only the higher luminosity compact double and GPS quasars (relativistically beamed emission) could expect to be detected. Even surveys that aim to improve our knowledge of the less luminous GPS source population, such as those by Snellen et al. (2004) or Peck and Taylor (2000), would struggle to detect PKS 2254–367 or NGC 1052 at distances $> 50 \text{ Mpc}$.

With only PKS 2254–367 and NGC 1052 to suggest the possibility of a low-luminosity, jet dominated population of GPS sources which is the analog of FR-I radio galaxies, it is important to collect further data for other nearby candidate objects. The information on NGC 1052 and PKS 2254–367 suggest a way forward. We should target

a sample of weak (10–100 mJy corresponding to luminosities of $10^{21-22} \text{ W Hz}^{-1}$ at distances of $\sim 10 - \sim 70 \text{ Mpc}$) radio sources in nearby elliptical galaxies. Such radio sources have been examined with rudimentary high resolution observations previously (e.g., Slee et al. 1994) but without examination of broad-band radio spectra (to find peaked spectra) or detailed imaging.

Some progress in this direction has been made by de Vries et al. (2009), who report VLBI observations of sources in the CORALZ sample of Snellen et al. (2004). An interesting example is J105731+405646 with a 1.4 GHz flux density of 47 mJy and a clearly peaked spectrum near 1.3 GHz. Snellen et al. give a redshift of 0.008, with a corresponding luminosity of $L = 10^{21.59} \text{ W Hz}^{-1}$ at 5 GHz, however a redshift of 0.025 is also given in the literature for this object (Miller et al. 2002). In any case, de Vries et al. find the object is unresolved in their EVN + VLBA observation, with an image peak of 14 mJy/beam at 5 GHz.

4 CONCLUSIONS

The nuclear radio sources in IC 1459 and NGC 1052 are remarkably similar, as are the properties of the host galaxies themselves. Both compact radio sources appear to have symmetric jets of approximately the same luminosity, much lower than typically noted in compact double GPS sources. Similarities between PKS 2254–367 and NGC 1052 and differences with respect to other GPS galaxies lead us to speculate that a sub-class of GPS radio sources, with low luminosity and with jet-dominated morphologies, exists and would be largely absent from previous radio source surveys. We suggest that a low-luminosity, jet-dominated population of GPS sources may be the analog of FR-I radio galaxies, with the higher luminosity lobe-dominated GPS sources being the analog of FR-II radio galaxies.

ACKNOWLEDGMENTS

We thank an anonymous referee for very useful comments on this manuscript that prompted significant improvements. The National Radio Astronomy Observatory is a facility of the National Science Foundation operated under cooperative agreement by Associated Universities, Inc. SJT acknowledges the support of the Western Australian State government, in the form of a Western Australia Premiers Fellowship.

REFERENCES

- Bettoni D., Galletta G., García-Burillo S., Rodríguez-Franco A., 2001, *A&A*, 374, 421
- Cappellari M., Verolme E. K., van der Marel R. P., Verdoes Kleijn G. A., Illingworth G. D., Franx M., Carollo C. M., de Zeeuw P. T., 2002, *ApJ*, 578, 787
- de Vries W. H., Barthel P. D., O’Dea C. P., 1997, *A&A*, 321, 105
- de Vries N., Snellen I. A. G., Schilizzi R. T., Mack K.-H., Kaiser C. R., 2009, *A&A*, 498, 641
- Edwards P. G., Tingay S. J., 2004, *A&A*, 424, 91
- Fanaroff B. L., Riley J. M., 1974, *MNRAS*, 167, 31P

- Forbes D. A., Franx M., Illingworth G. D., 1994, *ApJ*, 428, L49
- Gabel J. R., Bruhweiler F. C., Crenshaw D. M., Kraemer S. B., Miskey C. L., 2000, *ApJ*, 532, 883
- Giovannini, G., Cotton, W.D., Feretti, L., Lara, L. & Venturi, T. 2001, *ApJ*, 552, 508
- Labiano A., Barthel P. D., O’Dea C. P., de Vries W. H., Pérez I., Baum S. A., 2007, *A&A*, 463, 97
- Lister M. L., et al., 2013, *AJ*, 146, 120
- Meier D. L., Edgington S., Godon P., Payne D. G., Lind K. R., 1997, *Natur*, 388, 350
- Miller C. J., Krughoff K. S., Batuski D. J., Hill J. M., 2002, *AJ*, 124, 1918
- Murphy T., et al., 2010, *MNRAS*, 402, 2403
- O’Dea C. P., 1998, *PASP*, 110, 493
- Orienti, M., Dallacasa, D. & Stanghellini, C. 2007, *A&A*, 475, 813
- Orienti, M. et al. 2004, *A&A*, 426, 463
- Peck A. B., Taylor G. B., 2000, *ApJ*, 534, 90
- Readhead A. C. S., Taylor G. B., Pearson T. J., Wilkinson P. N., 1996, *ApJ*, 460, 634
- Sadler E. M., Ricci R., Ekers R. D., Sault R. J., Jackson C. A., de Zotti G., 2008, *MNRAS*, 385, 1656
- Shepherd M. C., 1997, *ASPC*, 125, 77
- Slee O. B., Sadler E. M., Reynolds J. E., Ekers R. D., 1994, *MNRAS*, 269, 928
- Snellen I. A. G., Mack K.-H., Schilizzi R. T., Tschager W., 2003, *PASA*, 20, 38
- Snellen I. A. G., Mack K.-H., Schilizzi R. T., Tschager W., 2004, *MNRAS*, 348, 227
- Tingay S. J., et al., 1997, *AJ*, 113, 2025
- Tingay S. J., et al., 2002, *ApJS*, 141, 311
- Tingay, S. J. et al., 2003a, *PASJ*, 55, 351
- Tingay, S. J., Edwards, P. G. & Tzioumis, A. K., 2003b, *MNRAS*, 346, 327
- Tingay S. J., et al., 2015, *AJ*, in press, arXiv:1412.4216
- Tingay S. J., de Kool M., 2003, *AJ*, 126, 723
- Tingay, S. J., Murphy, D. W., 2001, *ApJ*, 546, 210
- Verdoes Kleijn G. A., van der Marel R. P., Carollo C. M., de Zeeuw P. T., 2000, *AJ*, 120, 1221
- Vermeulen R. C., Ros E., Kellermann K. I., Cohen M. H., Zensus J. A., van Langevelde H. J., 2003, *A&A*, 401, 113
- Wilkinson P. N., Polatidis A. G., Readhead A. C. S., Xu W., Pearson T. J., 1994, *ApJ*, 432, L87
- Wu et al. 2013, *A&A* 550, 113
- Zwaan, M.A. et al. 2004, *MNRAS*, 350, 1210